IRS-Enabled Spectrum Sharing: Interference Modeling, Channel Estimation and Robust Passive Beamforming

GUAN Xinrong[1], WU Qingqing[2]

(1. College of Communications Engineering, Army Engineering University of PLA, Nanjing 210007, China;
2. State Key Laboratory of Internet of Things for Smart City, University of Macau, Macau 999078, China)

DOI: 10.12142/ZTECOM.202201005

https://kns.cnki.net/kcms/detail/34.1294.TN.20220303.1145.004.html, published online March 6, 2022

Manuscript received: 2021-11-11

Abstract: Intelligent reflecting surface (IRS), with its unique capability of smartly reconfiguring wireless channels, provides a new solution to improving spectrum efficiency, reducing energy consumption and saving deployment/hardware cost for future wireless networks. In this paper, IRS-enabled spectrum sharing is investigated, from the perspectives of interference modeling, efficient channel estimation and robust passive beamforming design. Specifically, we first characterize the interference in a spectrum sharing system consisting of a single primary user (PU) pair and a single secondary user (SU) pair, and extend it to the large-scale network by leveraging the Poisson point process (PPP). Then, we propose an efficient channel estimation framework based on decoupling the cascaded IRS channels. Moreover, the tradeoff between spectrum efficiency and energy efficiency is derived from the view of channel estimation accuracy. Finally, we discuss the robust passive beamforming design in presence of imperfect channel estimation and nonideal/discrete phase shifts. It is hoped that this paper provides useful guidance for unlocking the full potential of IRS for achieving efficient spectrum sharing for future wireless networks.

Keywords: intelligent reflecting surface; spectrum sharing; channel estimation; passive beamforming

Citation (IEEE Format): X. R. Guan and Q. Q. Wu, "IRS-enabled spectrum sharing: interference modeling, channel estimation and robust passive beamforming," *ZTE Communications*, vol. 20, no. 1, pp. 28–35, Mar. 2022. doi: 10.12142/ZTECOM.202201005.

1 Introduction

Over the past few decades, the rapid development of wireless applications and exponentially grown wireless devices have led to an ever-increasing demand for a high data rate and seamless coverage. To fulfill these requirements, a variety of wireless technologies have been proposed by academics and engineers, such as ultra-dense network (UDN), massive multiple-input multiple-output (MIMO), millimeter wave (mmWave) communication, and so on. However, for the future beyond fifth-generation (B5G) wireless network, it becomes insufficient to rely solely on the above technologies, when considering various emerging services and applications, such as 3D holographic imaging and presence, 5D communications (sight, hearing, touch, smell and taste), and the Internet of Everything (IoE), with more challenging performance requirements, e. g., 100 Gbit/s to 1 Tbit/s peak data rates, 100/m^3 device density, and 10 times more energy efficient than 5G[1]. For example, seeking more spectrum resources in the mmWave and even terahertz (THz) bands inevitably suffers from path loss and blockage. Though densely deployed base stations (BSs) and/or substantially increased antennas at the BSs can help to overcome the above problems, they are faced with practical challenges in terms of energy consumption, hardware cost and signal processing.

Recently, due to the developments in metamaterials/metasurfaces, intelligent reflecting surface (IRS) has emerged as an energy-efficient and cost-effective technology to solve the above problems[2–4]. Specifically, IRS is a planar surface consisting of a large number of passive reflecting elements, each of which can independently reflect the incident signal with a tunable phase and/or amplitude. By dynamically adjusting the reflecting coefficients to adapt to the wireless propagation environment, the signal can be enhanced/suppressed in desired/undesired directions. Since IRS requires no power-hungry components, e.g., radio frequency (RF) chains, it has the potential to achieve near-zero power consumption by exploiting wireless energy harvesting module[5]. Moreover, IRS can be integrated into existing wireless networks without changes at the transceivers, thus providing great flexibility in practical de-

Corresponding author: Wu Qingqing
The work of GUAN Xinrong was supported by the National Natural Science Foundation of China under Grant No. 62171461 and Natural Science Foundation on Frontier Leading Technology Basic Research Project of Jiangsu under Grant No. BK20212001. The work of WU Qingqing was supported by the Macau Science and Technology Development Fund, Macau SAR, under Grant Nos. 0119/2020/A3, SKL-IOTSC-2021-2023 and 0108/2020/A, the Guangdong NSF under Grant No. 2021A1515011900, and the Open Research Fund of National Mobile Communications Research Laboratory, Southeast University, under Grant No. 2021D15.

ployment. Owing to the above advantages, IRS has been extensively studied in various wireless systems, such as non-orthogonal multiple access (NOMA)[6–7], simultaneous wireless information and power transfer (SWIPT)[8–9], secrecy communications[10–12], and so on.

On the other hand, spectrum sharing has been thoroughly investigated in the literature as an efficient way to solve the spectrum scarcity problem, by fully exploiting the opportunities within the limited spectrum resource rather than resorting to higher frequency bands. Provided that the quality of service (QoS) for primary users (PUs) is ensured, secondary users (SUs) can share the same spectrum thus the spectrum efficiency can be significantly improved. However, the SU performance largely decreases in the presence of strong cross-link interference. For instance, considering a spectrum sharing communication system consisting of a pair of PU and a pair of SU, the SU rate would be constrained by the strong interference from PT if the primary transmitter is located near the secondary receiver. Alternatively, if the secondary transmitter is located near the primary receiver, the SU rate would also be constrained since the transmission power of the secondary transmitter should be tuned at an extremely low level for ensuring the reception at the primary receiver. As such, the spectrum sharing efficiency largely depends on the interference distribution. Note that with increased device density, the future wireless network will take the interference challenge to a new level, which will thus limit the application potential of spectrum sharing.

With capability for signal enhancement as well as interference suppression, IRS is a promising solution to tackling the above spectrum sharing challenges. Fig. 1 shows three typical setups for IRS-enabled spectrum sharing. In particular, in Setup 1, by deploying an IRS nearby the SU cluster, the interference from the primary BS (PBS) can be efficiently reduced at the SUs, while the desired signal from the secondary BS (SBS) can be enhanced. As such, the transmission power at the SBS can be largely decreased such that the QoS at the PUs can be guaranteed, even if PUs are located near the SBS. In Setup 2, an IRS is deployed nearby the SBS. In this case, the transmission of SBS can be properly tuned so that the signal/interference at the SUs/PUs can be enhanced/reduced. In Setup 3, considering that an IRS is deployed nearby the PU cluster. Then, by mitigating the SBS-PU interference, the SBS can enlarge its transmission power for combating the PBS's interference at the SUs.

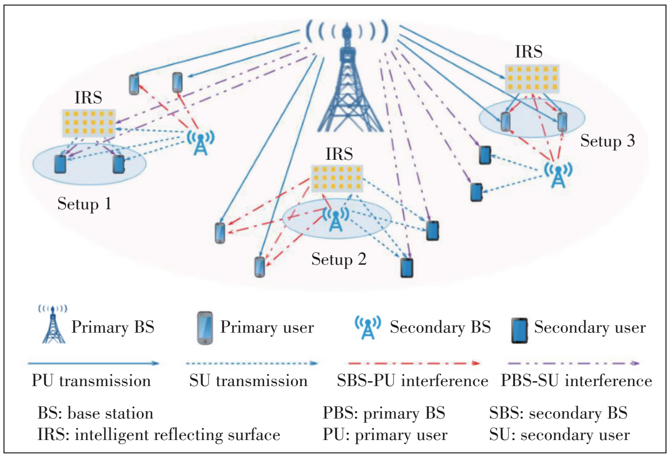

▲**Figure 1. IRS-enabled spectrum sharing with different setups**

However, most existing works focus on the IRS-aided point-to-point transmission or broadcast system, while its promising channel reconfiguration ability for spectrum sharing, i.e., interference channel, has not been well studied. Motivated by this, we investigate the IRS-enabled spectrum sharing, from the perspectives of interference modeling, efficient channel estimation and robust passive beamforming design. The main contributions of this work are summarized as follows. 1) An interference-based performance analysis model is established to evaluate the passive beamforming gain of IRS assisted spectrum sharing system. 2) An efficient channel estimation method based on decoupling the cascaded reflecting channel is proposed. Moreover, we derive the tradeoff between energy efficiency and spectrum efficiency from the perspective of channel estimation accuracy. 3) A robust passive beamforming design framework is proposed while considering the imperfect channel estimation and nonideal/discrete reflection coefficients in practice.

The rest of this paper is organized as follows. Section 2 presents an interference-based performance analysis model. Section 3 discusses the efficient channel estimation and Section 4 investigates the robust passive beamforming design. Section 5 provides the numerical results to evaluate the performance of the proposed designs. Finally, we conclude this paper in Section 6.

2 Interference Modeling

It is not easy to evaluate the passive beamforming gain of IRS in spectrum sharing systems due to the complicated links among PUs and SUs. However, considering that the bottleneck of spectrum sharing is the interference, starting from interference modeling is expected to provide some useful insights. Thus, in this section, we aim to characterize the performance gain of IRS from the view of interference. In particular, we first consider the IRS-enabled spectrum sharing system consisting of a single PU pair and a single SU pair, and then extend the analysis to the more general and practical large-scale network setup with massive users.

2.1 Case 1: Single PU Pair and Single SU Pair

Fig. 2 shows an IRS-enabled spectrum sharing system, where an SU link consisting of a secondary transmitter (ST) and a secondary receiver (SR) coexists with a PU link consisting of a primary transmitter (PT) and a primary receiver (PR), and an IRS is deployed to assist in the spectrum sharing. Assume that all nodes are equipped with a single antenna, while the number of reflecting elements at the IRS is denoted by N. The baseband equivalent channels from the PT(ST) to the PR,

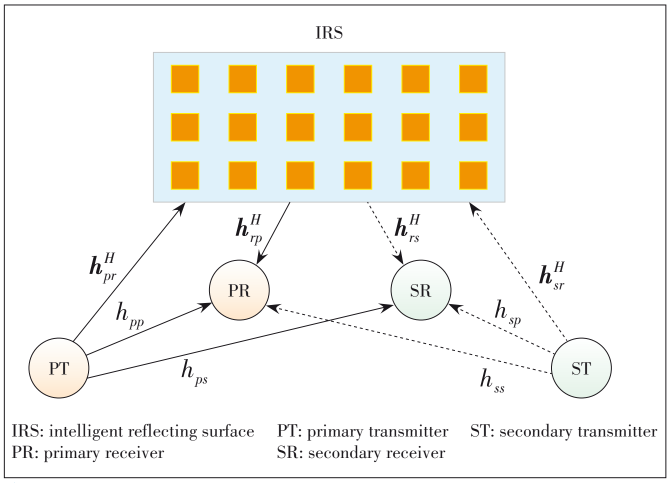

▲ **Figure 2. IRS-enabled spectrum sharing with single primary-user/secondary-user (PU/SU) pair**

SR and IRS are denoted by h_{pp}, h_{ps}, $\boldsymbol{h}_{pr} \in \mathbb{C}^{N \times 1}$, h_{sp}, h_{ss} and $\boldsymbol{h}^H_{sr} \in \mathbb{C}^{1 \times N}$, respectively, while those from the IRS to the PR and SR are denoted by $\boldsymbol{h}^H_{rp} \in \mathbb{C}^{1 \times N}$ and $\boldsymbol{h}^H_{rs} \in \mathbb{C}^{1 \times N}$, respectively. Let $\boldsymbol{v}^H = \left[v_1, v_2, ..., v_N \right]$ represent the passive beamforming vector of the IRS, where $v_n = e^{j\theta_n}$, $\theta_n \in [0, 2\pi)$ is the phase shift on the combined incident signal by its n-th element. The composite PT/ST-IRS-PR/SR channel is then modeled as a concatenation of three components, namely, the PT/ST-IRS link, the IRS reflecting with phase shifts, and the IRS-PR/SR link. The quasi-static flat-fading model is assumed for all channels. We assume that the channel state information (CSI) of all channels involved is perfectly known at the ST/IRS for the joint power control and passive beamforming design.

Assume that the transmission power at the PT and ST is given by p_p and p_s, respectively, while the complex additive white Gaussian noise (AWGN) at the PR and SR is denoted by $n_p \sim CN(0, \sigma_p^2)$ and $n_s \sim CN(0, \sigma_s^2)$, respectively. As a result, the received interference power at the PR and SR is respectively given by

$$\begin{cases} I_p = p_s \left| h_{sp} + \boldsymbol{v}^H \boldsymbol{h}_{srp} \right|^2 \\ I_s = p_p \left| h_{ps} + \boldsymbol{v}^H \boldsymbol{h}_{prs} \right|^2 \end{cases}, \tag{1}$$

where $\boldsymbol{h}_{srp} = \mathrm{diag}(\boldsymbol{h}^H_{rp}) \boldsymbol{h}^*_{sr}$ and $\boldsymbol{h}_{prs} = \mathrm{diag}(\boldsymbol{h}^H_{rs}) \boldsymbol{h}^*_{pr}$. Traditionally, since the interference at the PR, i.e., I_p should be constrained below a certain threshold such that the QoS at the PR can be ensured, the transmission power of ST, i.e., p_s should be very low in the presence of strong ST-PR link, which thus results in an extremely low SU data rate. Fortunately, by deploying an IRS, the above strong interference can be effectively mitigated with that from the reconfigurable reflecting channel. As such, the transmission power at the ST can be largely improved as well as the SU data rate.

Motivated by the above, we focus on the ST-PR interference I_p, of which the minimum value can be given by

$$\begin{aligned} I_p^{\min} &= \min_{\boldsymbol{v}} p_s \left| h_{sp} + \boldsymbol{v}^H \boldsymbol{h}_{srp} \right|^2, \\ &\text{s.t.} \left| v \right|_n = 1. \end{aligned} \tag{2}$$

It can be observed that the maximum power gain of the reflected channel can be expressed by

$$I_R = \max_{\boldsymbol{v}} \left| \boldsymbol{v}^H \boldsymbol{h}_{srp} \right|^2 = \left| \sum\nolimits_{n=1}^{N} \boldsymbol{h}_{srp}(n) \right|^2, \tag{3}$$

which represents the maximum capability of the IRS for interference mitigating. In particular, if $I_R \geqslant \left| h_{sp} \right|^2$, the interference at the PR can be completely reduced, i.e., $I_p^{\min} = 0$, via properly designed passive beamforming. Otherwise, the minimum interference at the PR is then given by

$$I_p^{\min} = p_s \left(\left| h_{sp} \right| - \left| \sum\nolimits_{n=1}^{N} \boldsymbol{h}_{srp}(n) \right| \right)^2. \tag{4}$$

2.2 Case 2: Large-Scale Network with Massive Users

In practical systems, the interference modeling would be much more complex due to massive users. In this subsection, we still focus on the interference at the PR side, which is crucial to the maximum allowed transmission power at STs. Fig. 3 shows IRS-enabled spectrum sharing in a large-scale network, where an IRS is deployed nearby the PR to reduce the interference from multiple STs. Denote the distances from PT to PR and IRS by d_{pp} and d_{pr}, respectively, that from IRS to PR by d_{rp}, and those from the i-th ST to PR and IRS by $d_{s_i p}$ and $d_{s_i r}$, respectively. Assuming that the distribution of STs in the considered circle area with radius R follows a Poisson point process (PPP) with density λ_s. Denoting the number of STs by K,

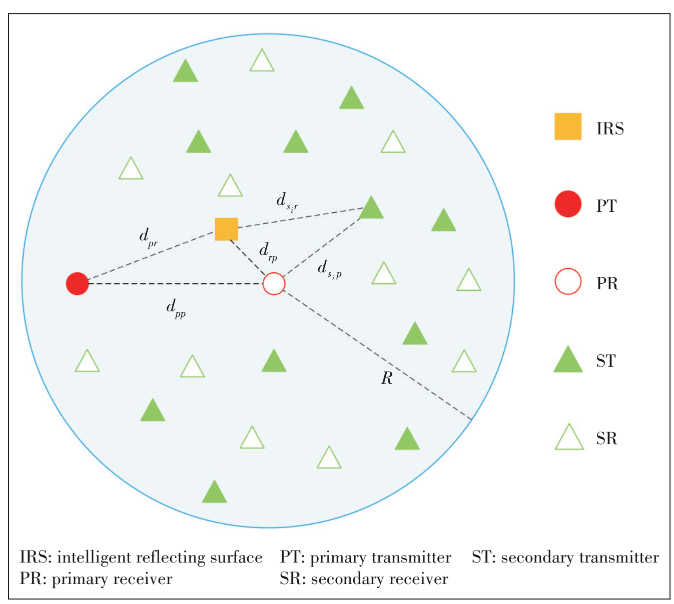

▲ **Figure 3. IRS-enabled spectrum sharing in large-scale network** the probability of K=k is then expressed by

$$\Pr(K = k) = e^{-\lambda_s \pi R^2} \left(\pi R^2\right)^k / k!, \quad k \geq 0. \tag{5}$$

Moreover, considering both the path loss and small-scale fading, the channels are given by

$$\boldsymbol{h}_{ij} = L_{ij} \boldsymbol{g}_{ij}, \ i \in \left\{p, s_i, r\right\}, j \in \left\{r, p\right\}, i \neq j, \tag{6}$$

where $L_{ij} = L_0 d_{ij}^{-c}$ denotes the path loss, L_0 is the path loss at a reference distance of 1 m, and c is the corresponding path loss exponent, while $\boldsymbol{g}_{ij}$ follows complex Gaussian distribution with zero means and unit variances. Based on the above, the power of total interference at the PR can be written as

$$I_p = \sum_{i=1}^{k} p_{s_i} \left| L_{s_i p} \boldsymbol{g}_{s_i p} + \sum_{n=1}^{N} L_{s_i r} L_{rp} \boldsymbol{g}_{s_i r}(n) \boldsymbol{g}_{rp}(n) v_n \right|^2. \tag{7}$$

It can be observed that the interference power I_p largely depends on a variety of distances, which are random variables themselves. To obtain the statistical characteristics of I_p, we first derive its eigenfunction by

$$\varphi_{I_p}(t) = \sum_{k=0}^{\infty} \Pr\{K = k\} \mathbb{E}\left(e^{jtI_p} \middle| k\right). \tag{8}$$

Then, by exploiting the Fourier transformation, the probability density function (PDF) of I_p can be obtained. Note that without IRS, the interference power I_p in Eq. (7) would be $I_p = \sum_{i=1}^{k} p_{s_i} \left| L_{s_i p} \boldsymbol{g}_{s_i p} \right|^2$. Comparing the PDF of I_p in two cases, some useful insights can be drawn into the performance gain of IRS for spectrum sharing.

3 Efficient Channel Estimation

In IRS-aided wireless systems, channel estimation is fundamentally challenging due to the following reasons[13]. First, the passive IRS elements can only reflect signals without the capability of signal transmission/reception, which thus makes the separate estimation of the BS-IRS and IRS-user channels infeasible. Alternatively, a practical approach is to estimate the cascaded BS-IRS-user channels based on the training signals from the BS/users with properly designed IRS reflection pattern over time[14]. Second, since the number of IRS reflecting elements is generally very large, the training overhead required for cascaded channel estimation becomes prohibitively high. To reduce the complexity, an element-grouping based channel estimation strategy was proposed in Ref. [15]. In particular, by grouping the adjacent IRS elements into a sub-surface, only the cascaded user-IRS-BS channel associated with each sub-surface needs to be estimated. Moreover, another approach to reduce the pilot overhead is exploiting the IRS channel sparsity, which however is usually applicable in the IRS-assisted communication system operating at high-frequency bands[16]. It should be noted that the above works cannot be straightforwardly extended to the IRS-aided multiuser system, since they mainly focus on channel estimation for the IRS-aided single-user system. As the number of users increases, the required pilot overhead becomes unaffordable by exploiting the above user-by-user successive channel estimation methods. Especially, for the IRS-enabled spectrum sharing system, in addition to increased transmission links, more interference links are involved, which further makes the channel estimation even more challenging.

In this section, we first propose an efficient channel estimation method for the IRS-enabled spectrum sharing system, which is motivated by the cascaded channel decoupling[17]. Then, we discuss the tradeoff between spectrum efficiency and energy efficiency.

3.1 Cascaded Channel Decoupling Based Channel Estimation

Take the IRS-enabled spectrum sharing system shown in Fig. 4 as an example, which consists of a multi-antenna PT, a multi-antenna ST, an IRS and multiple single-antenna PRs and SRs. It can be observed that: 1) All cascaded PT-IRS-PR/ST-IRS-SR channels share the common PT-IRS/ST-IRS channels. If such common channels can be obtained, only IRS-PR/IRS-SR channels need to be estimated for recovering the desired cascaded channels. Meanwhile, the training overhead can be largely reduced since the IRS-PR/IRS-SR channels are of much lower dimension as compared to the cascaded ones. 2) Since the locations of PT/ST and IRS are fixed, the above common channels usually vary much more slowly than the IRS-PR/IRS-SR channels, which thus only need to be esti-

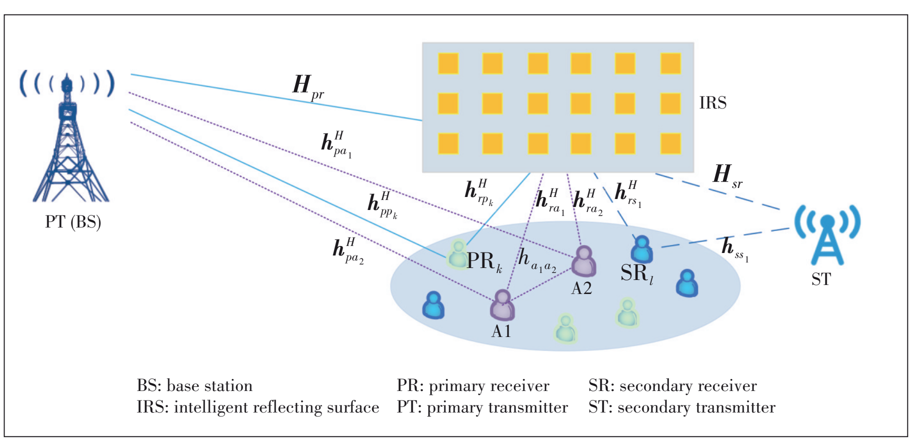

▲Figure 4. Cascaded channel decouple based channel estimation for IRS-enabled spectrum sharing system

mated offline. 3) Given the estimated PT-IRS/ST-IRS and IRS-SR/IRS-PR channels, the interference channels, i.e., PT-IRS-SR and ST-IRS-PR channels, can be directly obtained via computation, without additional training. Motivated by the above, we propose an efficient channel estimation method based on the cascaded channel decoupling, which is specified as follows and where the estimation of direct channels is omitted for brevity since the focus is the IRS involved channels.

3.1.1 Off-Line Estimation

As shown in Fig. 4, two anchor nodes, namely A1 and A2, are deployed nearby the IRS to assist in channel estimation in the considered IRS-enabled spectrum sharing system. First, A1 transmits pilot symbols, while PT, ST and A2 estimate $\boldsymbol{H}_{pra_1} = \mathrm{diag}(\boldsymbol{h}_{ra_1}^H)\boldsymbol{H}_{pr}$, $\boldsymbol{H}_{sra_1} = \mathrm{diag}(\boldsymbol{h}_{ra_1}^H)\boldsymbol{H}_{sr}$ and $\boldsymbol{h}_{a_1ra_2} = \mathrm{diag}(\boldsymbol{h}_{ra_1}^H)\boldsymbol{h}_{ra_2}^*$, respectively. Second, A2 feeds back the estimated $\boldsymbol{h}_{a_1ra_2}$ to PT and ST. Third, A2 transmits pilot symbols while PT and ST estimate $\boldsymbol{H}_{pra_2} = \mathrm{diag}(\boldsymbol{h}_{ra_2}^H)\boldsymbol{H}_{pr}$ and $\boldsymbol{H}_{sra_2} = \mathrm{diag}(\boldsymbol{h}_{ra_2}^H)\mathrm{H}_{sr}$, respectively. At last, based on the above estimated $\boldsymbol{H}_{pra_1}$, $\boldsymbol{h}_{a_1ra_2}$ and $\boldsymbol{H}_{pra_2}$, the separate PT-IRS, IRS-A1 and IRS-A2 channels can be obtained at PT[13]. Similarly, the ST-IRS channel can be obtained at ST based on the estimated $\boldsymbol{H}_{sra_1}$, $\boldsymbol{h}_{a_1ra_2}$ and $\boldsymbol{H}_{sra_2}$. Note that all of the above channels need to be estimated only once over a long time due to the fixed locations of the PT/ST, IRS and A1/A2.

3.1.2 On-Line Estimation

First, PRs consecutively transmit pilot symbols, while the PT estimates the IRS-PR channels efficiently by exploiting the offline estimated common PT-IRS channel. Then, the PT computes the desired PT-IRS-PR channels based on the offline estimated PT-IRS channel and the online estimated IRS-PR channel. Second, SRs consecutively transmit pilot symbols while the ST estimates the IRS-SR channels efficiently by exploiting the offline estimated common ST-IRS channel. After that, the ST can compute the desired ST-IRS-SR channels. Third, the PT and ST exchange the estimated IRS-PR and IRS-SR channels, such that they can obtain the CSI of the interference links, i. e., PT-IRS-SR/ST-IRS-PR without additional pilot training.

3.2 Tradeoff Between Spectrum Efficiency and Energy Efficiency

Obviously, a training-transmitting tradeoff is involved: too few training results in a coarsely estimated channel at the PT/ST and hence a reduced passive beamforming gain, whereas too much training costs excessive energy and also leaves less time for data transmission. To show the essential insight, we consider the IRS-enabled spectrum sharing system in Fig. 2 with single PU/SU pair for brevity. As shown in Fig. 5, assuming a channel coherence block of T_c (normalized by symbol duration), the time allocated for channel estimation and data transmission is denoted by T_e and T_d, respectively. Denoting the pilot power at PT/ST and the noise power by p_0 and σ_0^2, the mean-squared error (MSE) by applying the channel estimation method in Ref. [14] is given by $\sigma_0^2/\left(p_0 T_e\right)$. Thus, the channel estimation accuracy improves with larger p_0 and T_e, which thus leads to increased signal-to-interference-plus-noise ratio (SINR) at the PR and SR during the data transmission phase, i.e.,

$$\gamma_p\left(p_0, T_0\right), \gamma_s\left(p_0, T_0\right) \propto p_0, T_0. \tag{9}$$

Note that in spectrum sharing systems, PUs would not adapt their QoS requirement to SUs, while SUs should adjust their transmission strategy even towards a low data rate. If a QoS constraint on PU transmission as $\gamma_p\left(p_0, T_0\right) \geqslant \gamma_{th}$, where γ_{th} is the PU SINR target and corresponds to a fixed PU data rate $\log_2\left(1 + \gamma_{th}\right)$, the outage probability of PU transmission is obtained by $\Pr\{\gamma_p(p_0, T_0) < \gamma_{th}\}$. Based on the above, the average throughput of the spectrum sharing system during each T_c can be expressed by

$$\bar{\eta} = \left\{\Pr\left\{\gamma_p\left(p_0,T_0\right) \geqslant \gamma_{th}\right\}\log_2\left(1 + \gamma_{th}\right) + \log_2\left(1 + \gamma_s\left(p_0,T_0\right)\right)\right\}\left(1 - T_e/T_c\right). \tag{10}$$

One can observe that larger training time T_e on one hand results in lower outage probability for PU transmission and a higher data rate for SU transmission, but on the other hand renders a lower spectrum efficiency for leaving less time for data transmission.

Next, we consider the energy efficiency of the above channel estimation and data transmission protocol. The transmission power of the PT and ST in the data transmission phase is denoted by p_p and p_s, respectively, while the circuit power consumption in T_c (including that consumed in PT/PR/ST/SR/IRS) denoted by p_c. Thus, the system energy consumption in each T_c is given by

$$E = p_0 T_e + T_d\left(p_p + p_s\right) + T_c p_c. \tag{11}$$

Based on Eqs. (10) and (11), the energy efficiency can be obtained by

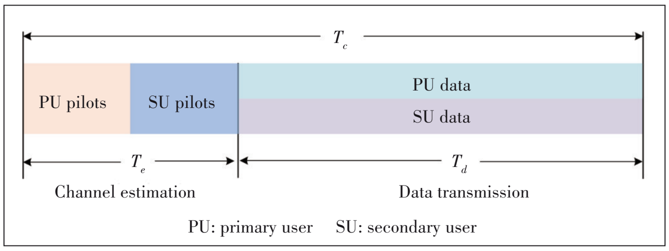

▲Figure 5. A channel estimation and data transmission protocol for the IRS-enabled spectrum sharing system in Fig. 2

$$\lambda = \frac{\bar{\eta}}{E} = \frac{\left\{\Pr\left\{\gamma_p\left(p_0, T_0\right) \geq \gamma_{th}\right\}\log_2\left(1+\gamma_{th}\right) + \log_2\left(1+\gamma_s\left(p_0, T_0\right)\right)\right\}\left(1 - T_e/T_c\right)}{p_0 T_e + T_d\left(p_p + p_s\right) + T_c p_c}. \quad (12)$$

Next, the tradeoff between spectrum efficiency and energy efficiency can be derived by

$$f = f\left(\bar{\eta}, E\right), \quad (13)$$

which can further be exploited to optimize the parameters settings, such as time/power allocation between the channel estimation phase and data transmission phase.

4 Robust Passive Beamforming Design

Most of the existing passive beamforming designs are based on the assumption of perfect CSI, which is however difficult to obtain in practice due to inevitable estimation errors arising from noise, feedback latency, limited pilot power, and so on[18]. Another assumption made in most existing works is that the IRS phase shifts optimized are continuous values, which is also challenging to implement in practice due to hardware limitations and cost control. Thus, implementing discrete and finite reflection phase shifts is more cost-effective. In this section, we propose robust passive beamforming designs with imperfect CSI and discrete phase shifts, respectively.

4.1 With Imperfect CSI

Considering the IRS-enabled spectrum sharing system shown in Fig. 2, we assume imperfect CSI for passive beamforming design. Denote $\bar{\boldsymbol{h}}_{ij}^T = [\boldsymbol{h}_{irj}, h_{ij}]$, $i,j \in \{p,s\}$ and $\bar{\boldsymbol{v}}^H = e^{j\omega}[\boldsymbol{v}^H, 1]$, while other notations are the same as those in Section 2. We assume that the CSI errors are bounded by some possible values, thus the channels are modeled by

$$\bar{\boldsymbol{h}}_{ij} = \hat{\boldsymbol{h}}_{ij} + \Delta\boldsymbol{h}_{ij}, \left\|\Delta\boldsymbol{h}_{ij}\right\|^2 \leq \xi, \quad (14)$$

where ξ is the radius of the uncertainty region. We aim to maximize the achievable SU rate via jointing the power control at the ST and the passive beamforming at the IRS, subject to the SINR constraint at the PR. Thus, the optimization problem is formulated as

$$\begin{aligned}
(\text{P1}):\ \max_{p_s, \bar{\boldsymbol{v}}}\ & \frac{p_s\left|\bar{\boldsymbol{v}}^H\left(\hat{\boldsymbol{h}}_{ss} + \Delta\boldsymbol{h}_{ss}\right)\right|^2}{p_p\left|\bar{\boldsymbol{v}}^H\left(\hat{\boldsymbol{h}}_{ps} + \Delta\boldsymbol{h}_{ps}\right)\right|^2 + \sigma_s^2} \\
\text{s.t.}\ & \frac{p_p\left|\bar{\boldsymbol{v}}^H\left(\hat{\boldsymbol{h}}_{pp} + \Delta\boldsymbol{h}_{pp}\right)\right|^2}{p_s\left|\bar{\boldsymbol{v}}^H\left(\hat{\boldsymbol{h}}_{sp} + \Delta\boldsymbol{h}_{sp}\right)\right|^2 + \sigma_p^2} \geq \gamma_{th}, \\
& p_s \leq P_{\max}, \left\|\Delta\boldsymbol{h}_{ij}\right\|^2 \leq \xi,\ i,j \in \{p,s\}, \\
& \left|\bar{v}_n\right| = 1, n = 1,\dots,N+1.
\end{aligned} \quad (15)$$

An alternating optimization (AO) based algorithm can be used to solve (P1) sub-optimally, by iteratively optimizing one of p_s and $\bar{\boldsymbol{v}}$ with the other being fixed at each iteration until the convergence is reached. Specifically, for given $\bar{\boldsymbol{v}}$, the optimal p_s can be easily obtained, whereas optimizing $\bar{\boldsymbol{v}}$ for given p_s is more challenging due to the channel estimation errors. By introducing variables t, α and β, (P1) can be rewritten as

$$\begin{aligned}
(\text{P2}):\ \max_{\bar{\boldsymbol{v}}}\ & t \\
\text{s.t.}\ & p_s\left|\bar{\boldsymbol{v}}^H\left(\hat{\boldsymbol{h}}_{ss} + \Delta\boldsymbol{h}_{ss}\right)\right|^2 \geq t\alpha, \\
& p_p\left|\bar{\boldsymbol{v}}^H\left(\hat{\boldsymbol{h}}_{ps} + \Delta\boldsymbol{h}_{ps}\right)\right|^2 + \sigma_s^2 \leq \alpha, \\
& p_p\left|\bar{\boldsymbol{v}}^H\left(\hat{\boldsymbol{h}}_{pp} + \Delta\boldsymbol{h}_{pp}\right)\right|^2 \geq \gamma_{th}\beta, \\
& p_s\left|\bar{\boldsymbol{v}}^H\left(\hat{\boldsymbol{h}}_{sp} + \Delta\boldsymbol{h}_{sp}\right)\right|^2 + \sigma_p^2 \leq \beta, \\
& \left\|\Delta\boldsymbol{h}_{ij}\right\|^2 \leq \xi, i,j \in \{p,s\}, \left|\bar{v}_n\right| = 1, n = 1,\dots,N+1.
\end{aligned} \quad (16)$$

Then, by exploiting S-procedure, the constraints involved with CSI errors can be re-expressed by a variety of linear matrix inequalities. Further, by leveraging the technique of semidefinite relaxation (SDR), the optimization problem (P2) can be solved.

4.2 With Discrete Phase Shifts

To focus on the discrete passive beamforming design, here we assume perfect CSI for brevity. Denoting the number of tunable IRS phase shift by Q, the set of discrete reflection coefficients for each IRS element can be written as $v_n \in \{0, e^{j\Delta\theta}, \dots, e^{j(Q-1)\Delta\theta}\}$, $n = 1,\dots,N$. We aim to maximize the achievable SU rate via jointly optimizing p_s and $\bar{\boldsymbol{v}}$, subject to the SINR constraint at the PR. Thus, the optimization problem can be modeled by

$$\begin{aligned}
(\text{P3}):\ \max_{p_s, \boldsymbol{v}}\ & \frac{p_s\left|h_{ss} + \boldsymbol{v}^H\boldsymbol{h}_{srs}\right|^2}{p_p\left|h_{ps} + \boldsymbol{v}^H\boldsymbol{h}_{prs}\right|^2 + \sigma_s^2} \\
\text{s.t.}\ & \frac{p_p\left|h_{pp} + \boldsymbol{v}^H\boldsymbol{h}_{prp}\right|^2}{p_s\left|h_{sp} + \boldsymbol{v}^H\boldsymbol{h}_{srp}\right|^2 + \sigma_p^2} \geq \gamma_{th}, \\
& p_s \leq P_{\max}, \\
& v_n \in \{0, e^{j\Delta\theta}, \dots, e^{j(2^Q - 1)\Delta\theta}\}, n = 1,\dots,N.
\end{aligned} \quad (17)$$

Similar to (P2), the above optimization problem can be solved by the AO based algorithm, and we also focus on optimizing $\bar{\boldsymbol{v}}$ for given p_s. Since an IRS usually consists of a large number of reflecting elements, exhaustive search becomes infeasible. By denoting $\bar{\boldsymbol{v}}^H = e^{j\omega}[\boldsymbol{v}^H\ 1]$, $\bar{\boldsymbol{h}}_{ij}^T = [\boldsymbol{h}_{irj}, h_{ij}]$, and $\mathbf{H}_{ij} =$

$p_i \bar{\boldsymbol{h}}_{ij} \bar{\boldsymbol{h}}_{ij}^T$, $i,j \in \{p,s\}$, (P3) can be rewritten as

$$
\begin{aligned}
\text{(P4)}: \max_{\bar{\boldsymbol{v}}} \quad & t \\
\text{s.t.} \quad & \bar{\boldsymbol{v}}^H \left(\boldsymbol{H}_{ss} - t\boldsymbol{H}_{ps}\right) \bar{\boldsymbol{v}} \geqslant t\sigma_s^2, \\
& \bar{\boldsymbol{v}}^H \left(\boldsymbol{H}_{pp} - t\boldsymbol{H}_{sp}\right) \bar{\boldsymbol{v}} \geqslant \gamma_{th}\sigma_p^2, \\
& v_n \in \{0, e^{j\Delta\theta}, \ldots, e^{j(2^Q-1)\Delta\theta}\}, n = 1, \ldots, N.
\end{aligned} \tag{18}
$$

This is an integer nonlinear program, which is still difficult to solve. Then, by denoting $\boldsymbol{G}_s = \boldsymbol{H}_{ss} - t\boldsymbol{H}_{ps}$, $\boldsymbol{G}_p = \boldsymbol{H}_{pp} - t\boldsymbol{H}_{sp}$, $f_s = \bar{\boldsymbol{v}}^H \boldsymbol{G}_s \bar{\boldsymbol{v}} - \left|h_{ss}\right|^2 + t\left|h_{ps}\right|^2$, and $f_p = \bar{\boldsymbol{v}}^H \boldsymbol{G}_p \bar{\boldsymbol{v}} - \left|h_{pp}\right|^2 + t\left|h_{sp}\right|^2$, we have $f_s = \sum_{i=1}^{N-1} \sum_{j=l+1}^{N} 2\left[\mathrm{Re}\left(\boldsymbol{G}_s(i,j)\right)\cos\left(\theta_j - \theta_i\right) - \mathrm{Im}\left(\boldsymbol{G}_s(i,j)\right)\sin\left(\theta_j - \theta_i\right)\right] + \sum_{i=1}^{N} \boldsymbol{G}_s(i,i) + 2\sum_{i=1}^{N} \left|\boldsymbol{G}_s(i,N+1)\left[\cos\left(\angle\boldsymbol{G}_s(i,N+1)\right)\cos\theta_i - \sin\left(\angle\mathbf{G}_s(i,N+1)\right)\sin\theta_i\right]\right.$ and $f_p = \sum_{i=1}^{N-1} \sum_{j=l+1}^{N} 2\left[\mathrm{Re}\left(\mathbf{G}_p(i,j)\right)\cos\left(\theta_j - \theta_i\right) - \mathrm{Im}\left(\mathbf{G}_p(i,j)\right)\sin\left(\theta_j - \theta_i\right)\right] + \sum_{i=1}^{N} \mathbf{G}_p(i,i) + 2\sum_{i=1}^{N} \left|\boldsymbol{G}_p(i,N+1)\right|\left[\cos\left(\angle\boldsymbol{G}_p(i,N+1)\right)\cos\theta_i - \sin\left(\angle\mathbf{G}_p(i,N+1)\right)\sin\theta_i\right]$. As such, the integer quadratic constraints in Eq. (17) can be transformed into integer linear constraints, i.e., (P4) can be re-expressed into an integer linear program (ILP), for which the globally optimal solution can be obtained by applying the branch-and-bound method.

5 Numerical Results

As shown in Fig. 6, to study the effectiveness of deploying IRS in a spectrum sharing system, we consider two different setups with strong cross link interference. Specifically, in Setup 1, P1 and P2 work as PT and PR, and S1 and S2 work as SR and ST (thus incurring strong PT-SR interference), while in Setup 2, P1 and P2 work as PR and PT, and S1 and S2 work as ST and SR (thus incurring strong ST-PR interference). We assume that the system operates on a carrier frequency of 750 MHz with the wavelength λ_c=0.4 m and the path loss at the reference distance d_0=1 m is given by L_0=−30 dB. Suppose that the IRS is equipped with a uniform planar array with 6 rows and 10 columns, and the element spacing is λ_d=3λ_c/8. The noise power is set as −105 dBm. The channels between PT/ST and IRS/PR/SR are assumed to be Rayleigh fading with the path loss exponents set as 3, whereas the channels between IRS and PR in Setup 1 and SR in Setup 2 are line of sight (LoS) with the path loss exponents set as 2. Besides, the case without IRS but with successive interference cancellation (SIC) at the SR for mitigating the interference from PT, i.e., (no-IRS, SIC at SR), is also considered for performance comparison and showing the benefit of using IRS.

Fig. 7 shows the achievable SU rate versus the maximum transmit power of the ST in the considered two setups. It can be observed that the case with IRS always achieves a higher SU rate than that of the (no-IRS, SIC at SR) design. Specifically, in Setup 1, using IRS not only cancels the interference from the PT(P1) to the SR(S1), but also enhances the desired signal from the ST(S2) to the SR(S1); while applying SIC at the SR can only achieve the former. Moreover, the SU rate for the case with IRS eventually saturates. The reason is that both the ST(S2) and the PR(P2) are not in the coverage of IRS and thus the interference from the ST(S2) to the PR(P2) cannot be reduced, which then constraints the transmitting power at the ST(S2). In Setup 2, the no-IRS design becomes ineffective, though SIC is applied at the SR(S2). This is because given the severe interference from the ST(S1) to the PR(P1), the former should keep silent to guarantee the reception of the latter. However, by applying the IRS, the above ST-PR interference can be efficiently reduced, thus the SU can access the spectrum and achieve a higher rate with increased transmit power.

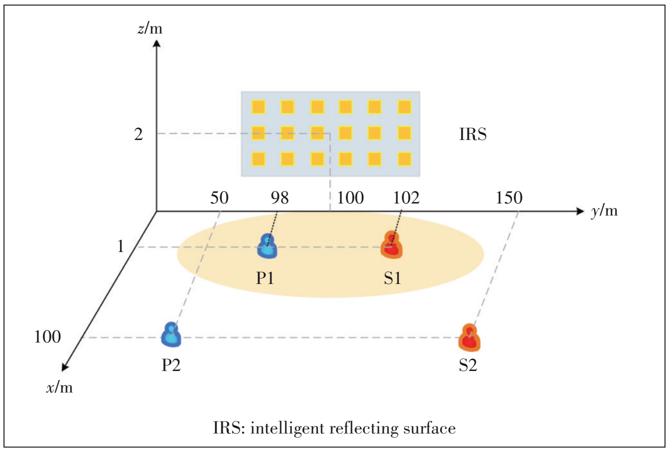

▲Figure 6. Two simulation setups with strong cross link interference

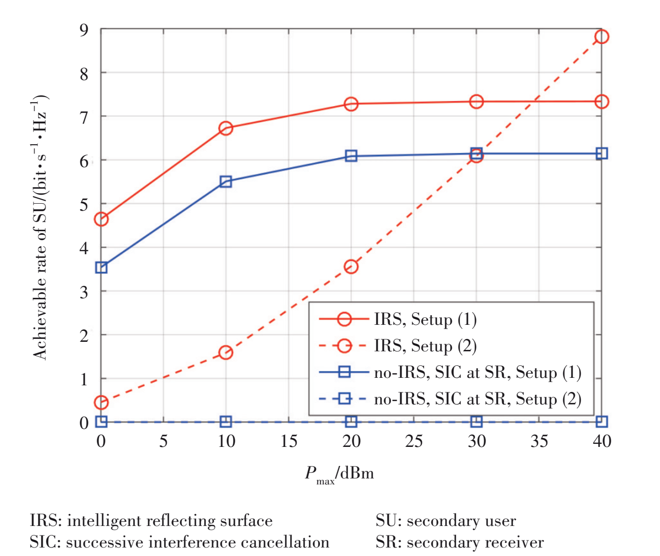

▲Figure 7. Achievable SU rate versus maximum transmitting power at secondary transmitter (ST)

6 Conclusions

IRS has been considered as a promising technology to achieve highly spectral and energy efficient wireless communication systems. In this paper, we investigate the IRS-enabled spectrum sharing system and highlight several important issues including the modeling of interference, estimation of channels and design of robust passive beamforming. Our simulations show the effectiveness of employing IRS to improve the SU rate and its advantages in dealing with highly challenging interference scenarios in conventional spectrum sharing systems without the IRS. We hope that this paper would provide a useful guidance for future research into this emerging and promising area.

References

[1] 6G Flagship. Key drivers and research challenges for 6G ubiquitous wireless intelligence [EB/OL]. (2019-09-09) [2021-10-14]. http://jultika. oulu. fi/Record/isbn978-952-62-2354-4
[2] WU Q Q, ZHANG R. Towards smart and reconfigurable environment: intelligent reflecting surface aided wireless network [J]. IEEE communications magazine, 2020, 58(1): 106 – 112. DOI: 10.1109/MCOM.001.1900107
[3] WU Q Q, ZHANG S W, ZHENG B X, et al. Intelligent reflecting surface aided wireless communications: a tutorial [J]. IEEE transactions on communications, 2021, 69(5): 3313–3351. DOI: 10.1109/TCOMM.2021.3051897
[4] LIU H, ZHANG J Y, WU Q Q, et al. RIS-aided next-generation high-speed train communications: challenges, solutions, and future directions [EB/OL]. (2021-03-17) [2021-10-14]. https://arxiv.org/abs/2103.09484
[5] WU Q, GUAN X, ZHANG R. Intelligent reflecting surface-aided wireless energy and information transmission: an overview [J]. Proceedings of the IEEE, 2021, 110(1): 150–170. DOI: 10.1109/JPROC.2021.3121790
[6] MU X, LIU Y, GUO L, et al. Exploiting intelligent reflecting surfaces in NOMA networks: joint beamforming optimization [J]. IEEE transactions on wireless communications, 2020, 19(10): 6884–6898. DOI: 10.1109/JPROC.2021.3121790
[7] DING Z, POOR H V. A simple design of IRS-NOMA transmission [J]. IEEE Communications Letters, 2020, 24(5): 1119–1123. DOI: 10.1109/LCOMM.2020.2974196
[8] WU Q Q, ZHANG R. Joint active and passive beamforming optimization for intelligent reflecting surface assisted SWIPT under QoS constraints [J]. IEEE journal on selected areas in communications, 2020, 38(8): 1735 – 1748. DOI: 10.1109/JSAC.2020.3000807
[9] PAN C H, REN H, WANG K Z, et al. Intelligent reflecting surface enhanced MIMO broadcasting for simultaneous wireless information and power transfer [J]. IEEE journal on selected areas in communications, 2020, 38(8): 1719 – 1734. DOI: 10.1109/JSAC.2020.3000802
[10] CUI M, ZHANG G C, ZHANG R. Secure wireless communication via intelligent reflecting surface [J]. IEEE wireless communications letters, 2019, 8(5): 1410–1414. DOI: 10.1109/LWC.2019.2919685
[11] SHEN H, XU W, GONG S L, et al. Secrecy rate maximization for intelligent reflecting surface assisted multi-antenna communications [J]. IEEE communications letters, 2019, 23(9): 1488–1492. DOI: 10.1109/LCOMM.2019.2924214
[12] ZHANG J Y, DU H Y, SUN Q, et al. Physical layer security enhancement with reconfigurable intelligent surface-aided networks [J]. IEEE transactions on information forensics and security, 2021, 16: 3480 – 3495. DOI: 10.1109/TIFS.2021.3083409
[13] JIN Y, ZHANG J, ZHANG X, et al. Channel estimation for semi-passive reconfigurable intelligent surfaces with enhanced deep residual networks [J]. IEEE transactions on vehicular technology, 2021, 70(10): 11083 – 11088. DOI: 10.1109/TVT.2021.3109937
[14] JENSEN T L, DE CARVALHO E. An optimal channel estimation scheme for intelligent reflecting surfaces based on a minimum variance unbiased estimator [C]// International Conference on Acoustics, Speech and Signal Processing (ICASSP). IEEE, 2020: 5000–5004. DOI: 10.1109/ICASSP40776.2020.9053695
[15] ZHENG B, ZHANG R. Intelligent reflecting surface enhanced OFDM: channel estimation and reflection optimization [J]. IEEE wireless communications letters, 2020, 9(4): 518–522. DOI: 10.1109/LWC.2019.2961357
[16] LIU H, ZHANG J, WU Q, et al. ADMM based channel estimation for RISs aided millimeter wave communications [J]. IEEE communications letters, 2021, 25(9): 2894–2898. DOI: 10.1109/LCOMM.2021.3095218
[17] GUAN X R, WU Q Q, Zhang R. Anchor-assisted channel estimation for intelligent reflecting surface aided multiuser communication [J]. IEEE transactions on wireless communications, 2021, early access. DOI: 10.1109/TWC.2021.3123674
[18] ZHANG J, ZHANG Y, ZHONG C, et al. Robust design for intelligent reflecting surfaces assisted MISO systems [J]. IEEE communications letters, 2020, 24 (10): 2353–2357. DOI: 10.1109/LCOMM.2020.3002557

Biographies

GUAN Xinrong received both the B.Eng. degree in communications engineering and Ph.D. degree in communications and information systems from the College of Communications Engineering, PLA University of Science and Technology, China in 2009 and 2014, respectively. From 2014, he worked as a lecturer at the College of Communications Engineering, Army Engineering University of PLA, China. His current research interests include physical layer security, wireless key generation, and intelligent reflecting surfaces. He has coauthored more than 40 IEEE papers with one ESI highly cited paper. He has served as a reviewer of several IEEE journals.

WU Qingqing (qingqingwu@um.edu.mo) received the B.Eng. and Ph.D. degrees in electronic engineering from South China University of Technology and Shanghai Jiao Tong University (SJTU), China in 2012 and 2016, respectively. He is currently an assistant professor with the State Key Laboratory of Internet of Things for Smart City, University of Macau, China. From 2016 to 2020, he was a research fellow in the Department of Electrical and Computer Engineering, National University of Singapore. His current research interests include intelligent reflecting surfaces, unmanned aerial vehicle (UAV) communications, and MIMO transceiver design. He has coauthored more than 100 IEEE papers with 23 ESI highly cited papers and eight ESI hot papers, which have received more than 9 000 Google citations. He was listed as a World's Top 2% Scientist by Stanford University in 2020 and a Clarivate ESI Highly Cited Researcher in 2021.